

# Semiempirical Hartree–Fock calculations for KNbO<sub>3</sub>

R. I. Eglitis,\* A. V. Postnikov, and G. Borstel

Universität Osnabrück – Fachbereich Physik, D-49069 Osnabrück, Germany

(Received 31 January 1996; revised manuscript received 10 April 1996)

In applying the semiempirical intermediate neglect of differential overlap (INDO) method based on the Hartree-Fock formalism to a cubic perovskite-based ferroelectric material KNbO<sub>3</sub>, it was demonstrated that the accuracy of the method is sufficient for adequately describing the small energy differences related to the ferroelectric instability. The choice of INDO parameters has been done for a system containing Nb. Based on the parametrization proposed, the electronic structure, equilibrium ground state structure of the orthorhombic and rhombohedral phases, and  $\Gamma$ -TO phonon frequencies in cubic and rhombohedral phases of KNbO<sub>3</sub> were calculated and found to be in good agreement with the experimental data and with the first-principles calculations available.

## I. INTRODUCTION

Potassium niobate, a perovskite-type ferroelectric material isostructural to barium titanate, has been subject to numerous *ab initio* electronic structure calculations during recent years. Earlier calculations have been performed for the ideal cubic perovskite structure in order to obtain electron band structure and to interpret optical<sup>1</sup> or x-ray photoelectron<sup>2</sup> spectra. Since then, special attention has been paid to the total energy calculations making it possible to determine the equilibrium geometry<sup>3,4</sup>, phonon frequencies<sup>5,6,7,8</sup>, and interatomic interaction parameters defining the ferroelectric phase transitions<sup>4,9</sup>.

Most of the calculations cited have been performed using the local density approximation (LDA), either with the pseudopotential method (Refs. 4 and 7) or with linearized augmented plane wave (Refs. 5, 8 and 10) or linearized muffin-tin orbital (LMTO, Refs. 3 and 6) method. The latter two approaches use some (different) forms of series expansions for the potential inside the muffin-tin spheres and in the interstitial. In the LDA-based calculation schemes, the potential is local and orbital independent, unless Coulomb correlation effects are *ad hoc* introduced by one or another implementation of self-interaction corrections,<sup>11</sup> or within the LDA+*U* (Ref. 12) formalism. This seems to be especially important for treating localized states, such as, e.g., those of transition-metal impurities in insulators. As has been shown in Ref. 13 for Fe in MgO, the straightforward implementation of a LDA scheme may lead to wrong results with respect to the energy positioning of impurity levels and the magnetic moment related to the impurity.

In contrast to LDA, the Hartree-Fock formalism automatically incorporates the dependence of the potential on the symmetry of a particular orbital, as well as on whether this orbital is occupied or not. Another convenient property of the Hartree-Fock formalism that is typically realized on a tight-binding basis set is that it can be more or less directly applied to crystal surfaces, providing correct asymptotics of the electron density at

the vacuum side.

*Ab initio* Hartree-Fock calculations are excessively computationally demanding (in the sense that quantitative results of comparable, or better, accuracy are in many cases obtainable within the LDA at much lower cost), therefore the applications to perovskite systems are not numerous. As an eventually single example, finite cluster Hartree–Fock calculation has been reported for a fragment of KNbO<sub>3</sub> structure.<sup>14</sup> However, a simplification on top of the Hartree–Fock method known as intermediate neglect of the differential overlap<sup>15,16</sup> (INDO) lets to decrease the computational effort considerably, at the price of treating several parameters as fitting variables, to be defined from outside the calculation scheme. In contrast to model calculations, which usually require an *ad hoc* fitting, the INDO parameters are believed to be largely transferable, so that, once determined for some chemical constituent, they may be successfully applied in the calculations for a variety of chemical substances where the latter participates.

Typical fields of INDO applications include various defects systems based on silica,<sup>15,17</sup> ionic oxides, such as MgO,<sup>15,16</sup> corundum,<sup>18,19</sup> zirconia,<sup>20</sup> or alkali halides.<sup>16,21</sup> The choice of INDO parameters is not a straightforward procedure but rather a trial-and-error loop, aimed at reproducing reasonably well band structure, equilibrium geometry, and characteristic energy differences for molecules or crystals, as based on experimental measurements or *ab initio* calculations. The list of parameters for several elements is given in Refs. 15 and 16 along with some discussion on the parameter optimization for ionic crystals.

The aim of the present paper is to demonstrate that the semiempirical INDO method may work well for perovskite-type ferroelectrics, and to provide the optimized set of INDO parameters for all constituents of KNbO<sub>3</sub>. Perovskites are generally expected to present a problem for any parametrized method, because of varying degree of covalency depending on chemical composition and because of strong polarizability of transition metal–oxygen bonds. An additional difficulty related to fer-

roelectric perovskites is that the energy differences that play a role in stabilizing the ferroelectric distorted structure, due to a fine balance between long-range Coulomb forces and short-range chemical bonding, have the order of magnitude of 1 mRy per formula unit or smaller, i.e., much lower than  $\sim 1$  eV energy differences being discussed, e.g., in relation to charged defects in silica.<sup>17</sup> Since this is the first, to our knowledge, application of the INDO method to perovskite systems, the question is to be answered whether the accuracy of the parametrized INDO method is sufficient to describe the ferroelectric instability, and whether the description of the underlying energetics is reliable. We optimize the INDO parameter set based on the comparison with available *ab initio* calculation results and experiments, and answer the above question positively by presenting the INDO calculations for atomic displacement patterns and phonon frequencies that are in good agreement with experimental data.

The paper is organized as follows. In Sec. II, we describe the essential features of the INDO method and the meaning of underlying parameters. In Sec. III, the choice of the INDO parameters used in our calculation is specified, based on the comparison with total energy *ab initio* calculations and the experimental structure data for KNbO<sub>3</sub>. In Sec. IV, atomic coordinates in the room-temperature orthorhombic phase and in the low-temperature rhombohedral phase are found by the total-energy-based structure optimization, and the results of INDO calculations for  $\Gamma$ -TO phonon frequencies are discussed.

## II. INDO METHOD AND PARAMETER OPTIMIZATION

The calculation scheme of the Hartree-Fock-Roothaan method in the INDO approximation is discussed in detail in Refs. 15 and 16. Basically, the procedure reduces to diagonalizing the matrix of the Fock operator to get the one-electron energies, and the linear combination of matrix elements with appropriate weights, depending on the occupation of corresponding one-electron states, provides the total energy. The fixed basis set is minimal in the sense that each of the atom-centered functions related to the valence-band states (4 in total per oxygen atom, 9 per transition-metal atom) is encountered only once. The construction of the on-site and off-diagonal parts of the Fock matrix is determined in terms of several empirical parameters, labeled by the atom type  $A$  and the index of the atomic orbital (AO)  $\mu$  (see Ref.<sup>15</sup>). The interaction of an electron in the  $\mu$ th valence AO on atom  $A$  with its own core

$$U_{\mu\mu}^A = -E_{\text{neg}}^A(\mu) - \sum_{\nu \in A} (P_{\nu\nu}^{(0)A} \gamma_{\mu\nu} - \frac{1}{2} P_{\nu\nu}^{(0)A} K_{\mu\nu})$$

contains, apart from the  $\zeta_\mu$  value, which specifies the Slater exponent for a one-exponential basis function and

hence Coulomb and exchange integrals  $\gamma_{\mu\nu}$  and  $K_{\mu\nu}$ , the initial guesses for the diagonal elements of the density matrix  $P_{\mu\mu}^{(0)A}$  and for the energy of the  $\mu$ th AO  $E_{\text{neg}}^A(\mu)$ , i.e., the ion's electronegativity. The interaction of the  $\mu$ th AO with the core of another atom  $B$  is approximated as

$$V_\mu^B = Z_B \{1/R_{AB} + [\langle \mu\mu | \nu\nu \rangle - 1/R_{AB}] \exp(-\alpha_{AB} R_{AB})\},$$

where  $R_{AB}$  is the distance between atoms  $A$  and  $B$ ,  $Z_B$  is the core charge of atom  $B$ , and parameter  $\alpha_{AB}$  describes the non-point character of this interaction.

Finally, the resonance-integral parameter  $\beta_{\mu\nu}$  enters the off-diagonal Fock matrix elements for the spin component  $u$ :

$$F_{\mu\nu}^u = \beta_{\mu\nu} S_{\mu\nu} - P_{\mu\nu}^u \langle \mu\mu | \nu\nu \rangle,$$

where the  $\mu$ th and  $\nu$ th AO are centered at different atoms,  $S_{\mu\nu}$  is the overlap matrix between them, and  $\langle \cdot | \cdot \rangle$  are two-electron integrals. Parameters  $\zeta_\mu$ ,  $\beta_{\mu\nu}$ ,  $\alpha_{AB}$  and  $E_{\text{neg}}^A(\mu)$  are usually fixed throughout the iterations, whereas  $P_{\nu\nu}^{(0)A}$  may be corrected as the self-consistency is being achieved.

It is in principle possible to implement the calculation in such way that the diagonalization is done for a number of  $\mathbf{k}$  vectors per iteration. However, conventional usage of the INDO method, given the low symmetry and possibly the lack of translation invariance in the systems it is usually applied to, restricts the diagonalization to the  $\Gamma$  point of the Brillouin zone only, taking instead a supercell, or large unit cell (LUC), all atoms of which contribute to the expanded basis set. For ideal systems, the enlargement of the unit cell is equivalent to increasing the density of the  $\mathbf{k}$  mesh in band-structure calculations, since the  $\Gamma$  point of the reduced (in the supercell) Brillouin zone maps onto different points of the original Brillouin zone of the single cell. For defect systems, there is no problem to treat, e.g., discrete impurity states in the dielectric gap, if one or few impurity atoms are included along with tens of bulk atoms in the LUC, since the  $\mathbf{k}$  dispersion of such states is negligible. Anyway, the enlargement of the unit cell in case of defect systems increases the variational freedom of the basis set.

Since the construction of the parametrized Fock matrix is straightforward, the bottleneck of the method in what regards the performance and accuracy is the diagonalization of large matrices. Compared to precise LDA-based schemes, such as, e.g., full-potential (FP) LMTO, which usually employ multiple-tail representation of basis functions,<sup>22,23</sup> the INDO method manages to handle considerably larger supercells. Compared to efficient minimal-basis computational schemes as, e.g., tight-binding LMTO,<sup>24</sup> INDO may exhibit such advantages as unrestricted spatial form of the potential, absence of muffin-tin boundary conditions, and of space-packing empty spheres.

As a method essentially based on the Hartree-Fock approximation, INDO does not provide a convenient option

to incorporate correlation effects into one-electron equations, as may be to some extent done within the LDA by an appropriate choice of the exchange-correlation potential. As a result, the dielectric band gap comes out in INDO overestimated usually by 3–5 eV (see, e.g., Ref. 15 and 18). Moreover, the lack of correlation effects, which imply some additional repulsion between electrons, overestimates the chemical binding and results in even more underestimated equilibrium bond lengths than is known to be the case in LDA calculations. Some part of correlation corrections (usually referred to as short-range corrections as they are mostly of intra-atomic nature) may be, however, incorporated in the choice of INDO parameters, since the latter are based on experimental or other external information anyway, and this may to some extent improve the two shortcomings mentioned.

### III. PARAMETER OPTIMIZATION

In the choice of INDO parameters for our calculation, we relied on the experimental information available and on the data of *ab initio* calculations for KNbO<sub>3</sub> (cited in Sec. I), which essentially agree in the description of the band structure. Whereas INDO calculations for many oxides and potassium salts have been done earlier, and the corresponding parameters for O and K tabulated,<sup>16</sup> no INDO calculations involving Nb have been, to our knowledge, done by now, so one-center and all involved two-center parameters had to be found. Since  $E_{\text{neg}}$  is related to the central energy position of an AO in question which is hybridized with many other states throughout the valence band, we calculated partial density of states (DOS) by sampling over a single ( $\Gamma$ )  $\mathbf{k}$  point in a LUC consisting of  $2 \times 2 \times 2$  or  $3 \times 3 \times 3$  single perovskite cells (40 or 135 atoms in total, correspondingly) and fitted to corresponding partial DOS from a LMTO calculation.  $\beta_{\mu\nu}$  affects the resonance interaction of the  $\mu$ th AO with other states and hence the width of the corresponding hybridized bands, which can be as well fitted to the *a priori* known partial DOS. We used for the two-center parameter  $\beta_{\mu\nu}$  a weighted value  $(\beta_{\mu} + \beta_{\nu})/2$ , therefore  $\beta_{\mu}$  and  $\beta_{\nu}$  may be calibrated in such a case as one-center parameters. For an initial value of  $P^{(0)}$ , an expected occupation of individual AO's, based on electronegativity considerations, in the compound in question may be taken, and then refined in the course of iterations. The two-center parameter  $\alpha_{AB}$ , which does not depend on orbital indices, plays a relatively minor role in what regards the band structure and DOS and affects primarily the energetics of atomic displacements, equilibrium bond lengths, and hence the equilibrium geometry. Finally,  $\zeta_{\mu}$ , nominally being a Slater exponent parameter and as such tabulated for all elements, should of course be considered here as a free parameter, which is used to improve the quality of our fixed, single-exponent basis set. It needs some adjustment based on a compromise between differ-

ent properties that are sought to be optimized.

An example of the total DOS per 135-atom LUC of KNbO<sub>3</sub> is shown in Fig. 1 along with the result of FP-LMTO calculation. The most obvious discrepancy is in the energy separation between the primarily O 2s band and the primarily O 2p+Nb 4d valence band. This difference is due to the neglect of self-interaction in the LDA-based LMTO calculation and the lack of correlation effects in the INDO; the experimental x-ray photoelectron measurements set O 2s–O 2p separation at about 15 eV,<sup>2</sup> halfway between the results of Hartree–Fock and LDA calculations. The experimental estimate of the optical gap of 3.3 eV (Ref. 25) is again in between the LDA value of 1.4 eV and 6.1 eV from the INDO calculation.<sup>26</sup> These differences have a physical foundation and cannot be removed without attributing unreasonable values to, e.g., O 2s and O 2p-related INDO parameters.

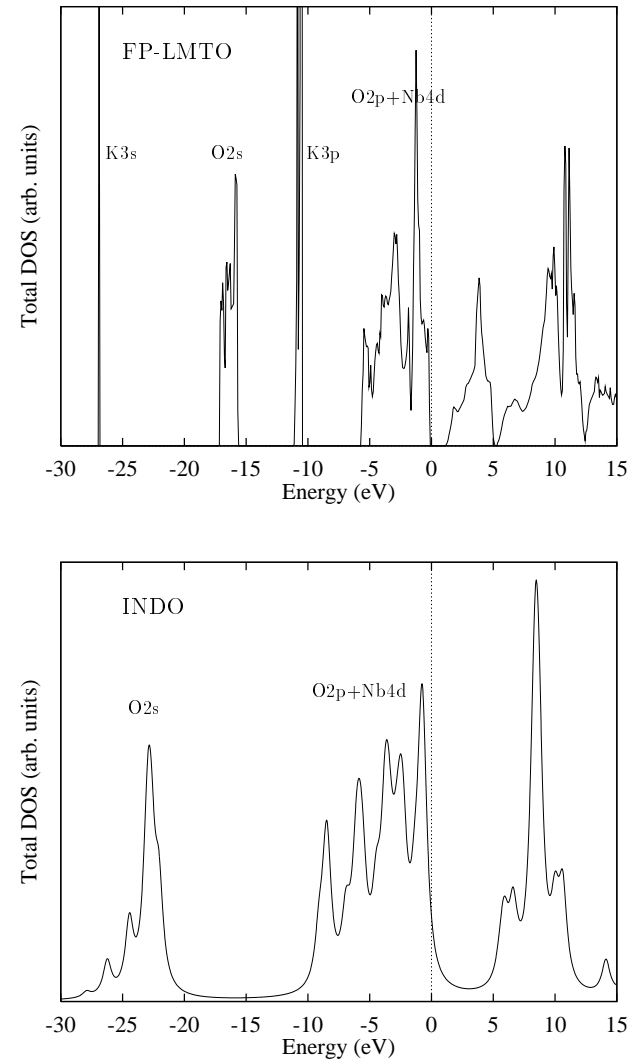


FIG. 1. Total density of states of KNbO<sub>3</sub> calculated with full-potential LMTO method (above) and INDO method for a  $3 \times 3 \times 3$  supercell (below). Energy scale is relative to the valence band top.

TABLE I. One-center INDO parameters

Orbital	$\zeta$ (a.u. $^{-1}$ )	$E_{\text{neg}}$ (eV)	$-\beta$ (eV)	$P_0$ (a.u.)
O 2s	2.27	4.5	16.0	1.974
O 2p	1.86	-12.6	16.0	1.96
Nb 5s	2.05	0.0	30.0	0.1
Nb 5p	2.05	-2.0	30.0	0.0
Nb 4d	1.60	23.85	16.0	0.6
K 4s	1.10	2.8	2.0	0.1
K 4p	1.25	0.3	3.0	0.03

The effective charges found by the Mullikan population analysis are +0.543 for K, +2.019 for Nb, and -0.854 for O. This is generally in agreement with simple tight-binding calculations,<sup>27</sup> but emphasizes higher degree of covalency of the K-O bond than may be expected from intuitive electronegativity considerations. One should note, however, that static effective charges are not well-defined properties and vary considerably depending on a method used.

K 3s and K 3p states, which were included into the valence-band basis set in the LMTO calculation, have been treated as core states in the INDO method. We found that in order to obtain correct equilibrium volume, it is essential to treat K 3p states as the basis AO's within the valence band, since their overlap with AO's of other atoms is not negligible. This observation is in agreement with what was earlier established in FP-LMTO calculations.<sup>3</sup> However, the inclusion of K 3p at the expense of K 4p in the minimal one-exponential basis of the INDO method does not allow one to describe off-center displacements and phonon frequencies with sufficient accuracy. Therefore, we prefer to keep the K 4p as a valence AO and to perform the calculations discussed below at the experimental lattice parameters of KNbO<sub>3</sub>.

Keeping in mind the necessity to obtain reliable values of equilibrium atomic displacements and the shape of the potential surface related to such displacements for subsequent studies of ferroelectric materials, we concentrated on these values as primary criteria for the quality of the INDO parametrization we look for. It is known that the fine balance between long-range electrostatic dipole-dipole interaction and the short-range chemical bonding effects is accountable for the ferroelectric instability, therefore the parameters  $\alpha_{AB}$  and  $\beta_\mu$  were especially subject to refinement, once  $E_{\text{neg}}$  and  $P^{(0)}$  are essentially fixed based on a band-structure analysis. The total-energy results from the INDO calculations for different displacement patterns have been fitted to analogous data obtained earlier with the FP-LMTO method as described in Ref. 3. We made sure that the optimized parameter set provides reasonable agreement with the FP-LMTO data in describing different displacement patterns and is not confined to any particular symmetry.

Since the shape of the total-energy hypersurface over atomic displacements is not directly measurable experimentally, and the results by different *ab initio* calculation

schemes differ somehow in determining the depth and the position of the off-center potential minima (see, e.g., Refs. 5 and 10), we relied also on a neutron-diffraction data concerning the displaced atomic positions in the ferroelectric phases of KNbO<sub>3</sub>,<sup>28</sup> and on the  $\Gamma$  transverse-optic (TO) phonon frequencies as additional reference points to test our parametrization. The one-center INDO parameters we found to provide the best compromise in reproducing all these properties are given in Table I. The best-fitted two-center parameters  $\alpha_{AB}$  are 0.15, 0.33 and 0.39 a.u. $^{-1}$  for A=O and B=O, Nb and K, correspondingly, and zero for A=Nb and K. The results of our ground-state geometry and phonon calculations are discussed in the next section.

## IV. RESULTS AND DISCUSSION

### A. Sequence of ferroelectric phases

As the temperature lowers, KNbO<sub>3</sub> undergoes a sequence of phase transitions from paraelectric cubic to ferroelectric tetragonal then orthorhombic then rhombohedral phases. The atomic positions in all these phases have been determined by Hewat.<sup>28</sup> As a first approximation, each of these ferroelectric phases is characterized by the off-center displacement of the Nb atom from its symmetric position in the cubic perovskite cell along [100], [110], or [111] in three subsequent ferroelectric phases, with the gradual lowering of the total energy. On top of this major distortion, K and O atoms somehow adjust their positions as compatible with the reduced symmetry of each particular phase, and a lattice strain eventually appears. The hierarchy of total-energy lowerings

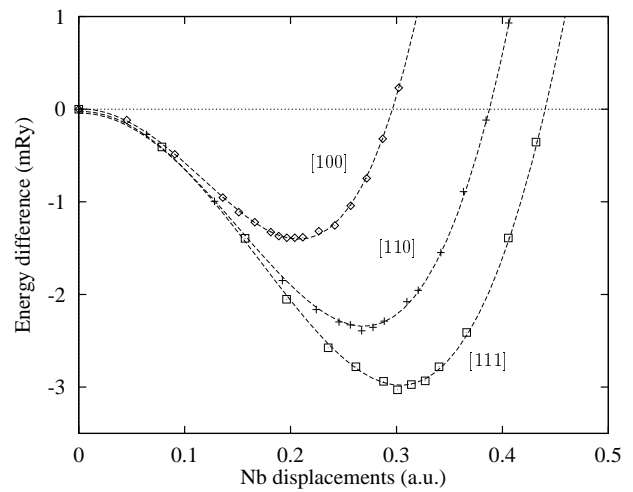


FIG. 2. Total energy as a function of off-center Nb displacements along different directions from its position in the cubic perovskite structure as calculated with the INDO ( $2 \times 2 \times 2$  supercell) method.

TABLE II. Calculated  $\Gamma$ -TO frequencies and eigenvectors in cubic  $\text{KNbO}_3$ .

Symmetry	Eigenvectors (present work)					$\omega$ calc. ( $\text{cm}^{-1}$ )				$\omega$ expt. ( $\text{cm}^{-1}$ )	
	K	Nb	O	O	O	Present	Ref. 5	Ref. 6	Ref. 7	Ref. 32	Ref. 33
$T_{1u}$	0.05	-0.57	0.70	0.30	0.30	292 <i>i</i>	115 <i>i</i>	203 <i>i</i>	143 <i>i</i>	96	115
$T_{1u}$	-0.88	0.34	0.21	0.16	0.16	178	168	193	188	198	207
$T_{1u}$	-0.02	-0.19	-0.61	0.54	0.54	537	483	459	506	521	522
$T_{2u}$	0	0	0	1	-1	272	266	234		280 <sup>a</sup>	

<sup>a</sup> Measurements at 585 K (in the tetragonal phase), Ref. 32.

related to the Nb displacements along three directions is therefore an important benchmark for the quality of the calculation in question. In Fig. 2, the energy gain due to the Nb displacements from the central position in the cubic perovskite cell (with the lattice constant  $a=3.997 \text{ \AA}$ ) is shown as calculated by the INDO method for the  $2 \times 2 \times 2$  supercell.

As is consistent with the experimental data, the [111] displacement and hence the rhombohedral phase provides the lowest ground-state energy, followed by the [110] displacement (orthorhombic phase) and the [100] displacement (tetragonal phase). This qualitative result is relatively stable against some variations of the INDO parameters. As regards the magnitudes of the off-center displacements and the depth of the related total-energy wells, our INDO parametrization (Table I) provides good agreement with the results of the FP-LMTO calculations accounting to all three displacement directions [see Fig. 4(a) of Ref. 3 and Fig. 1(b) of Ref 9].

### B. $\Gamma$ -TO frozen phonons in the cubic phase

As another test for the quality of our INDO parametrization for the adequate description of the atomic-displacement potential surface, we calculated the  $\Gamma$  TO phonon frequencies in the cubic phase of  $\text{KNbO}_3$ . Similar calculations have been done earlier by other methods,<sup>5,6,8</sup> and the experimental data (obtained mostly by infrared reflectivity measurements<sup>32,33</sup>) are available. We performed the calculations for a lattice constant  $a = 3.997 \text{ \AA}$  (that is based on an experimental perovskite cell volume extrapolated to zero temperature) within a conventional frozen-phonon scheme, using the  $2 \times 2 \times 2$  LUC. Consistently with the symmetry analysis given, e.g., in Ref. 6, we studied the effect on the calculated total energy of small coupled distortions compatible with the  $T_{1u}$  irreducible representation, that reveals three TO frequencies, and of the oxygen displacement within the single “silent” mode compatible with the  $T_{2u}$  irreducible representation of the  $Pm3m$  space group. The calculated phonon frequencies and eigenvectors are given in Table II.

The calculated frequencies generally fall within the limits set by previous *ab initio* calculations,<sup>5,6,7</sup> with somehow better agreement for the hard  $T_{1u}$  mode and the  $T_{2u}$  mode. The eigenvectors agree well with those calcu-

lated in Ref. 5 by the FP-LAPW method (for the lattice constant  $a = 4.016 \text{ \AA}$ ), and with those calculated in Ref. 6 by FP-LMTO. Anyway, the main pattern of atomic vibrations within each particular  $T_{1u}$  mode (primarily Nb displacement in the soft mode; almost pure K vibration against all other atoms in the intermediate mode, and the stretching of the oxygen octahedra in the hard mode) are correctly reproduced. The detailed structure of the soft mode eigenvector reveals smaller participation of K in the displacements with respect to the center of mass than was obtained in the FP-LMTO calculation.<sup>6</sup> This seems to be consistent with the atomic coordinates in the tetragonal phase that emerges as the soft mode freezes down (see Ref. 28 for the experimental data, and Fig. 1 of Ref. 6), and this behavior comes out correctly based on our INDO parametrization.

### C. Equilibrium displacements in the orthorhombic phase

As an additional benchmark for the fine adjustment of two-center INDO parameters, we aimed at obtaining a possibly good agreement with the experimental data<sup>28</sup> in determining all atomic positions, and not only the Nb displacement, in the orthorhombic and rhombohedral ferroelectric phases. The orthorhombic phase is important because it exists in a broad temperature range around room temperature and is subject to most studies and practical applications. The rhombohedral phase is specially discussed below. Keeping the lattice vectors for the orthorhombic phase fixed and equal to those listed in Ref. 28 ( $a=3.973 \text{ \AA}$  along  $\mathbf{x} = [100]$  of the cubic aristotype,  $b=5.695 \text{ \AA}$  along  $\mathbf{y} = [011]$  and  $c=5.721 \text{ \AA}$  along  $\mathbf{z} = [011]$ ), we allowed the  $c$  relaxation of K and Nb atoms and the  $b$  relaxation of those O atoms that are in the same [001] plane with Nb in the course of INDO calculations towards self-consistency. The total-energy minimization is implemented in the code making use of the downhill simplex method (see, e.g., Ref. 30). The resulting atomic positions within the orthorhombic cell are shown in Table III in comparison with the neutron-diffraction estimations of Ref. 28. It was of course our aim to provide as good agreement as possible by an appropriate choice of INDO parameters, but the encouraging result is that the agreement is very good, given the small number of parameters

TABLE III. Positions of atoms in orthorhombic and rhombohedral phases of  $\text{KNbO}_3$  (in terms of lattice parameters) as determined by neutron diffraction measurements, Ref. 28, and optimized in the INDO calculation.

Atom	$a$	$b$	$c$		$\Delta_{exp}$	$\Delta_{calc}$
Orthorhombic phase						
K	0	0	$\Delta_z$			0.0209
Nb	$\frac{1}{2}$	0	$\frac{1}{2}$			
O <sub>I</sub>	0	0	$\frac{1}{2} + \Delta_z$			0.0347
O <sub>II</sub>	$\frac{1}{2}$	$\frac{1}{4} + \Delta_y$	$\frac{1}{4} + \Delta_z$	}	$\Delta_z :$	0.0342 $\pm$ 9
O <sub>II</sub>	$\frac{1}{2}$	$\frac{3}{4} - \Delta_y$	$\frac{1}{4} + \Delta_z$		$\Delta_y :$	-0.0024 $\pm$ 9
Rhombohedral phase						
K	$\Delta_z$	$\Delta_z$	$\Delta_z$			0.0139
Nb	$\frac{1}{2}$	$\frac{1}{2}$	$\frac{1}{2}$			
O	$\frac{1}{2} + \Delta_x$	$\frac{1}{2} + \Delta_x$	$\Delta_z$	}	$\Delta_x :$	0.0213
O	$\frac{1}{2} + \Delta_x$	$\Delta_z$	$\frac{1}{2} + \Delta_x$		$\Delta_z :$	0.0328
O	$\Delta_z$	$\frac{1}{2} + \Delta_x$	$\frac{1}{2} + \Delta_x$			

that are not directly related to the structure properties. The most noticeable discrepancy is in the relative displacement of K atoms, which was somehow overestimated as compared with the experimental value; the similar trend obtained in the FP-LMTO optimization of the orthorhombic phase was much more pronounced.<sup>31</sup> One should note that the error in determining the position by neutron scattering is, of all atoms involved, maximal for K,<sup>28</sup> and that our present estimate falls within the error bars given in Ref. 28.

#### D. Displacements and phonons in the rhombohedral phase

The rhombohedral phase corresponds to the low-temperature ground-state structure of  $\text{KNbO}_3$ , which is what any zero-temperature total-energy minimization should normally drive at, with all structural constraints lifted. We looked for optimized atomic positions compatible with the symmetry of the rhombohedral phase, using the lattice constants of  $a=b=c=4.016$  Å (Ref. 28) but keeping the rhombohedral strain angle fixed. The reason for this was that the total energy was found to be very insensitive to the rhombohedral strain in  $\text{BaTiO}_3$  in a FP calculation by Cohen and Krakauer,<sup>29</sup> and we do not expect to achieve better accuracy for  $\text{KNbO}_3$  in our INDO calculation. Moreover, we neglected the deviation of the rhombohedral strain angle  $\alpha = 89.83^\circ$  from  $90^\circ$ .

The experimental and our optimized atomic positions in terms of lattice vectors are given in Table III. This is, to our knowledge, the first optimization of the atomic positions in the rhombohedral phase of  $\text{KNbO}_3$ . The maximal discrepancy with the experiment is for the  $\Delta_x(\text{O})$  parameter that describes a slight stretching of oxygen octahedra. This parameter is obviously related to the rhombohedral strain and may be slightly adjusted in a calculation incorporating the exact value of the strain angle. The relative displacements of K, Nb, and O along

the polar [111] axis are all found to be in very good agreement with the experiment. The quality of the description of the total-energy hypersurface in the rhombohedral phase was further controlled by calculating the  $\Gamma$  TO-phonon frequencies. The general symmetry relations between the  $\Gamma$  phonon modes in the cubic and rhombohedral phases may be found, e.g., in Ref. 32. We consider in the present work only three  $A_1$  modes, which originate from the  $T_{1u}$  block of the cubic phase, as the crystal symmetry lowers and all the soft modes become stabilized. The calculated frequencies and eigenvectors are given in Table IV. The components of the eigenvector related to K and Nb displacement exist only along [111], whereas each of three equivalent O atoms may also have the normal component of the displacement, in the threefold axial symmetry along the polar axis. The experimental phonon frequency data for the rhombohedral phase do not seem to be numerous; the values shown in Fig. 8 of Ref. 32 are about 200, 270 and 600  $\text{cm}^{-1}$ . Our calculated frequencies are in good agreement with these data. It is interesting to compare the eigenvectors with those for the cubic structure. One can see that the “pure K” mode is not affected by the structure transformation, preserving almost exactly its frequency and the displacement pattern. The former soft mode of the cubic phase only slightly changes the eigenvector, but gets hardened up to 278  $\text{cm}^{-1}$  in the rhombohedral structure. Finally, the highest-frequency mode has the lowest contribution of K and Nb displacements and is essentially related to the stretching of the oxygen octahedra, as in the cubic phase.

#### V. SUMMARY

In applying the semiempirical INDO method to the study of a cubic perovskite system, we demonstrated that the method is sufficiently sensitive for the adequate description of a ferroelectric instability. The energy gain of the order of  $\sim 1$  mRy per unit cell, i.e., much lower

TABLE IV. Calculated frequencies and eigenvectors of the  $\Gamma$ - $A_1$  modes in rhombohedral KNbO<sub>3</sub>.

$\omega$ (cm <sup>-1</sup> )	Eigenvectors			
	K <sub>  [111]</sub>	Nb <sub>  [111]</sub>	O <sub>  [111]</sub>	O <sub>⊥[111]</sub>
173	0.88	-0.37	-0.16	0.04
278	0.03	-0.53	0.40	0.28
593	0.04	0.26	-0.23	0.51

than one has to deal with in other conventional applications of the INDO method, are nevertheless reliably reproduced, resulting in a correct description of the microscopic structure of ferroelectric orthorhombic and rhombohedral phases and of the  $\Gamma$  TO-phonon frequencies and eigenvectors. The choice of the INDO parameters was proposed for the Nb-containing system, and may be used in further applications.

## ACKNOWLEDGMENTS

The work has been done as part of the German-Israeli joint project “Perovskite-based solid solutions and their properties.” Financial support by the Niedersächsische Ministerium für Wissenschaft und Kultur and by the Deutsche Forschungsgemeinschaft (SFB 225) is gratefully acknowledged. The authors are grateful to Yu. F. Zhukovskii and E. A. Kotomin for helpful discussions.

\* On leave from Institute of Solid State Physics, University of Latvia, Riga, Latvia.

<sup>1</sup> Yong-Nian Xu, W. Y. Ching, and R. H. French, *Ferroelectrics* **111**, 23 (1990).

<sup>2</sup> T. Neumann, G. Borstel, C. Scharfschwerdt, and M. Neumann, *Phys. Rev. B* **46**, 10623 (1992).

<sup>3</sup> A. V. Postnikov, T. Neumann, G. Borstel, and M. Methfessel, *Phys. Rev. B* **48**, 5910 (1993).

<sup>4</sup> R. D. King-Smith and D. Vanderbilt, *Phys. Rev. B* **49**, 5828 (1994).

<sup>5</sup> D. J. Singh and L. L. Boyer, *Ferroelectrics* **136**, 95 (1992).

<sup>6</sup> A. V. Postnikov, T. Neumann, and G. Borstel, *Phys. Rev. B* **50**, 758 (1994).

<sup>7</sup> W. Zhong, R. D. King-Smith, and D. Vanderbilt, *Phys. Rev. Lett.* **72**, 3618 (1994).

<sup>8</sup> R. Yu and H. Krakauer, *Phys. Rev. Lett.* **74**, 4067 (1995).

<sup>9</sup> S. Dorfman, D. Fuks, A. Gordon, A. V. Postnikov, and G. Borstel, *Phys. Rev. B* **52**, 7135 (1995).

<sup>10</sup> D. J. Singh, *Ferroelectrics* **164**, 143 (1995).

<sup>11</sup> J. P. Perdew and A. Zunger, *Phys. Rev. B* **23**, 5048 (1981); A. Svane and O. Gunnarsson, *Phys. Rev. Lett.* **65**, 1148 (1990).

<sup>12</sup> V. I. Anisimov, J. Zaanen, and O. K. Andersen, *Phys. Rev. B* **44**, 943 (1991); A. I. Liechtenstein, V. I. Anisimov, and J. Zaanen, *Phys. Rev. B* **52**, R5467 (1995).

<sup>13</sup> M. A. Korotin, A. V. Postnikov, T. Neumann, G. Borstel, V. I. Anisimov, and M. Methfessel, *Phys. Rev. B* **49**, 6548 (1994).

<sup>14</sup> H. Donnerberg and M. Exner, *Phys. Rev. B* **49**, 3746 (1994).

<sup>15</sup> A. Shluger, *Theoret. Chim. Acta (Berl.)* **66**, 355 (1985).

<sup>16</sup> E. Stefanovich, E. Shidlovskaya, A. Shluger, and M. Zakharov, *phys. stat. sol.(b)* **160**, 529 (1990).

<sup>17</sup> A. Shluger and E. Stefanovich, *Phys. Rev. B* **42**, 9664 (1990).

<sup>18</sup> P. W. M. Jacobs, E. A. Kotomin, A. Stashans, E. V. Stefanovich, and I. Tale, *J. Phys. Condens. Matter* **4**, 7531 (1992).

<sup>19</sup> E. A. Kotomin, A. Stashans, L. N. Kantorovich, A. I. Lifshitz, A. I. Popov, I. Tale, and J.-L. Calais, *Phys. Rev. B* **51**, 8770 (1995).

<sup>20</sup> E. V. Stefanovich, A. L. Shluger, and C. R. A. Catlow, *Phys. Rev. B* **49**, 11560 (1994).

<sup>21</sup> A. L. Shluger and E. A. Kotomin, *Phys. Status Solidi B* **108**, 673 (1981).

<sup>22</sup> M. Methfessel, *Phys. Rev. B* **38**, 1537 (1988).

<sup>23</sup> S. Yu. Savrasov and D. Yu. Savrasov, *Phys. Rev. B* **46**, 12181 (1992).

<sup>24</sup> O. K. Andersen, Z. Pawłowska, and O. Jepsen, *Phys. Rev. B* **34**, 5253 (1986).

<sup>25</sup> E. Wiesendanger, *Ferroelectrics* **6**, 263 (1974).

<sup>26</sup> The gap region is smeared up in the lower panel due to the broadening introduced while constructing the DOS by sampling.

<sup>27</sup> L. Douillard, F. Jollet, C. Bellin, M. Gautier, and J. P. Durraud, *J. Phys. Condens. Matter* **6**, 5039 (1994).

<sup>28</sup> A. W. Hewat, *J. Phys. C* **6**, 2559 (1973).

<sup>29</sup> R. E. Cohen and H. Krakauer, *Phys. Rev. B* **42**, 6416 (1990).

<sup>30</sup> W. H. Press, B. P. Flannery, S. A. Teukolsky, and W. T. Vetterling, *Numerical Recipes: the Art of Scientific Computing* (Cambridge University Press, New York, 1986).

<sup>31</sup> A. V. Postnikov and G. Borstel, *Phys. Rev. B* **50**, 16403 (1994).

<sup>32</sup> M. D. Fontana, G. Métrat, J. L. Servoin, and F. Gervais, *J. Phys. C* **17**, 483 (1984).

<sup>33</sup> F. Gervais, Y. Luspin, J. L. Servoin, and A. M. Quittet, *Ferroelectrics* **24**, 285 (1980).